Ubiquitous presence of intermolecular CH…O hydrogen bonds in as-synthesized zeolite materials

Shadi Al-Nahari, Karima Ata, Tzonka Mineva* and Bruno Alonso*
ICGM, Univ. Montpellier, CNRS, ENSCM, Montpellier, France.

CH…O hydrogen bonds (HBs) are identified in all crystals of series of silica zeolites hosting cationic Organic Structure Directing agents. This finding is supported by experimental C-O distances and COSi angles' distributions, and DFT calculations on representative structures. New insights are reported on the geometry and electrostatics of these HBs.

Weak hydrogen bonds (HBs) involving CH bonds as donor groups and O as acceptor atoms have been evidenced and described for several organic, biological and organometallic molecules, and have a recognized role in the formation and stabilization of many molecular and supramolecular assemblies.[1-6] In zeolite chemistry, CH…O HBs have been scarcely investigated. They have been identified between cationic organic structure directing agents (OSDAs) and silica frameworks (FWs) occasionally for some as-synthesized clathrates[7, 8] or zeolites,[9] but they are largely neglected until now when considering OSDA-zeolite intermolecular interactions. Using variable temperature IR spectroscopy and *ab initio* dynamics simulation, we have recently investigated the presence and characteristics of CH…O HBs in silicalite-1 (MFI) containing tetrapropylammonium cations and fluorine atoms.[10] This study allowed to evidence 28 weak CH…O HBs that represent 30% of the energy of the Coulomb electrostatic interaction between OSDA and the MFI zeolite framework. From these preliminary works, it appears to us that the presence of this type of HBs can be a general property of as-synthesised zeolites as there is no reason *a priori* that these interactions are not playing a role in similar chemical systems. This is what we wanted to verify by studying the widest possible series of OSDA-zeolite structures, and an appropriate selection of DFT optimised model structures.

Inspection of the available structures in crystallographic databases[‡] revealed a limited number of sets of chemically similar OSDA-zeolite structures. Among them, we chose to investigate first a full series found for 19 pure and non-defective silica structures presenting defined positions for F atoms (fluoride route) and non-protonated ammonium organocations $C_xH_yN_z^{n+}$ with different charge density as OSDAs (list in **ESI 1**). This choice allows to focus on the presence of CH…O interactions for a series presenting the wanted diversity in FW and OSDA types, avoiding side questions about the presence of strong HBs (e.g. NH…O) or the uncertainties on the location of negative charges (e.g. using hydroxide routes). Moreover, the conclusions drawn here from this first series can be extended to a series of structures of different composition (*vide infra*).

As hydrogen atoms are not, or not precisely, located in most of the available crystal structures, we exploited C, O and Si atomic positions. Indeed, distances between C and O atoms d_{CO} can give a strong indication about the presence of CH…O HBs. From Desiraju and Steiner work,[2] $d_{CO} \leq 3.3$ Å demonstrates the formation of these HBs, but longer distances (up to 4.0 Å) can also be considered for CH...O HBs. The analysis of the 19 silica-F-$C_xH_yN_z^{n+}$ zeolites allows to extract 19 individual distributions in d_{CO} and d_{CSi} (C-Si distances) further combined into two distributions presented in **Fig. 1**. These average distributions form almost continuous curves that are representative of the 19 individual distributions (**ESI 2**). A gradual increase in frequency counts is observed when increasing d_{CO} and d_{CSi} as well as a decrease when approaching the limit considered for the distributions (5 Å). We are therefore probing the first shell of C atoms close to the silica FW. The first conclusion we can draw is the presence of a significant proportion of cases (35 %) for $d_{CO} \leq 4$ Å, and a small but non-negligible proportion (4 %) for $d_{CO} \leq 3.3$ Å. It is to note that 15 structures over 19 present at least one CO moieties verifying $d_{CO} \leq 3.3$ Å, and all of them present $d_{CO} \leq 3.5$ Å. Herein, the existence of CH...O HBs can be confirmed, although the alternative presence of H...O van der Waals (vdW) interactions cannot be ruled out at this stage for $d_{CO} > 3.3$ Å. The second conclusion is that the d_{CSi} distribution start at higher values (~3.6 Å) than the d_{CO} distribution. It can be argued again that this is an effect of vdW interactions owing to the differences in vdW radii beween O and Si (1.52 and 2.10 Å respectively[11]). Nevertheless, by inspecting each structure, we found always for a given C atom (considered in these distributions) an O atom that is closer to C than to a Si atom. Therefore $d_{CO} < d_{CSi}$ is always obeyed, and there is no case showing a preferential proximity of C towards Si.

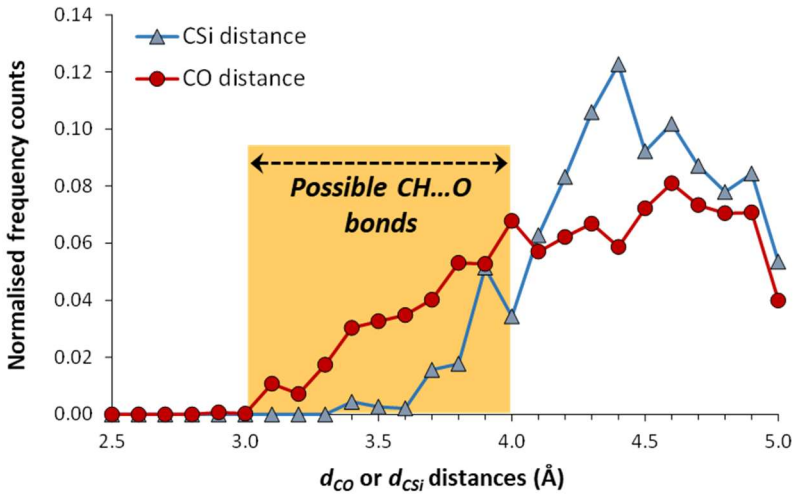

Fig. 1. C-O and C-Si distance distributions for the series of 19 silica-F-$C_xH_yN_z^{n+}$ zeolite structures.

One property of HBs is their directionality.[12] In the case of weak HBs, this property allows to distinguish them from vdW interactions.[13] For the experimental crystal structures, we addressed this question of directionality by analysing d_{CO} as a function of the distribution in COSi angles, for the SiOSi siloxane bonds involving O (contour lines in **Fig. 2**). This distribution is clearly not random for the d_{CO} range explored (2.5-5.0 Å) on the

contrary to what is obtained at higher d_{CO} values for which COSi angles take all possible values with a mean at 90° (example in **ESI 3**). Herein the interactions involving C, H and O atoms have a directional character and can be ascribed to HBs. In the contour map, a maximum in density is found for a COSi angle of 95° and d_{CO} = 4.0 Å. But subtle variations can be noticed by analysing the angle distribution as a function of d_{CO}. For a given d_{CO} interval, the COSi angle distribution follows a normal law (Gaussian fits in **Fig. 2**). The width of these distributions decreases when d_{CO} shortens while their centre deviates more from 90°. For the smallest d_{CO} (3 ±0.25 Å) – related to the strongest CH…O HBs – the highest probability is obtained for COSi angles of 104.4 ±0.2°. It is important to note that exactly the same conclusions on d_{CO}, d_{CSi} and COSi angles distributions are deduced for a second series of 11 silica-$C_xH_yO_wN_z^{n+}$ crystal structures not containing F and with a larger variety of OSDAs (**ESI 4**). This strengthen the widespread formation of CH…O HBs in OSDA-zeolite assemblies, and shows that this formation does not depend on the chemical composition of the negatively charged FW.[§]

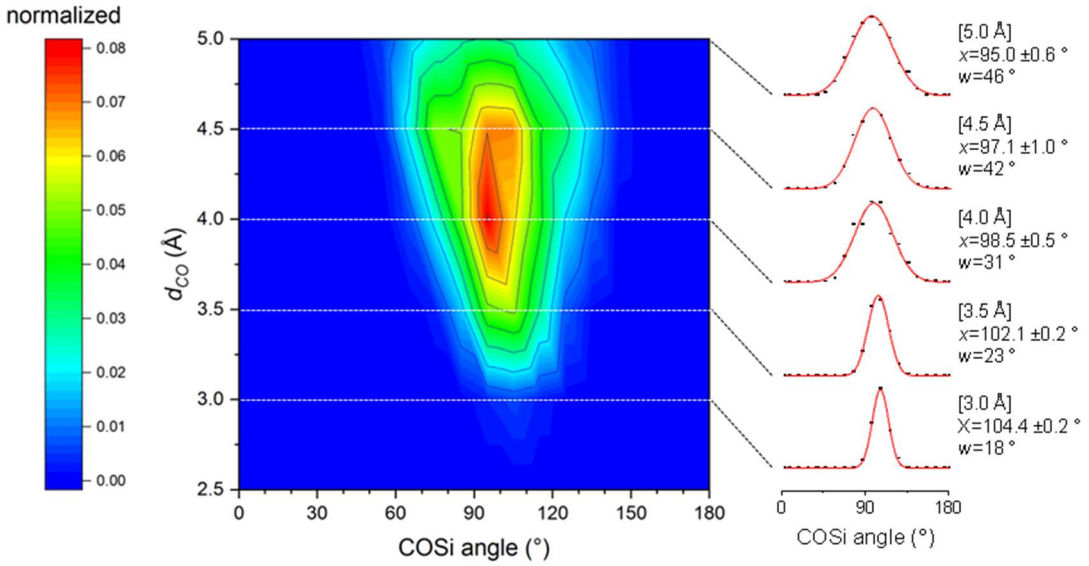

Fig. 2. COSi angles and d_{CO} distributions for the series of 19 silica-F-$C_xH_yN_z^{n+}$ zeolite structures presented as a density plot (frequency counts average over 5390 values). On the right, the graphs represent the angle distribution for a given d_{CO} value ±0.25 Å. The data are fitted with Gaussian functions (red curves) obtained by fitting. The centre and the width of the fitted distributions (*x* and *w* respectively) are given.

Other insights are gained when analysing the relationship between the two COSi angles related to one C close to one SiOSi bond (**ESI 5**). The differences between these angles tend to decrease when d_{CO} shortens. This means that C atoms become very close to the bisector plane of the SiOSi bonds when approaching O atoms. Concomitantly, the means of the two related COSi angles tend to a narrow range of values: 105-110°. These two observations from published crystal structures allow to build a model for the shortest CO distances. It is to note that the average bisector angle for SiOSi bonds in the series of 19 structures is 74° (±5°). Therefore, any X atom coplanar with these bonds and belonging to the bisector plane would have a XOSi angle of 106° in average, and this value is within the COSi values that can be extrapolated from the distributions in **Fig. 2**

and **ESI 5** for d_{CO} < 3 Å, corresponding to the strongest CH...O bond. This means that the related C atoms tend to locate within the SiOSi plane. Considering that the strongest CH...O bonds would have CHO angles close to 180°, the resulting geometrical model for these bonds in zeolites that can be extrapolated from the angular measurements is presented in **Scheme 1**. Obviously, a strict coplanarity between all atoms has little chance to exist given the complex interplay of intra- and intermolecular interactions in the as-synthesized zeolites but this extrapolated model is not far to what is also observed in the DFT optimised structures (*vide infra*).

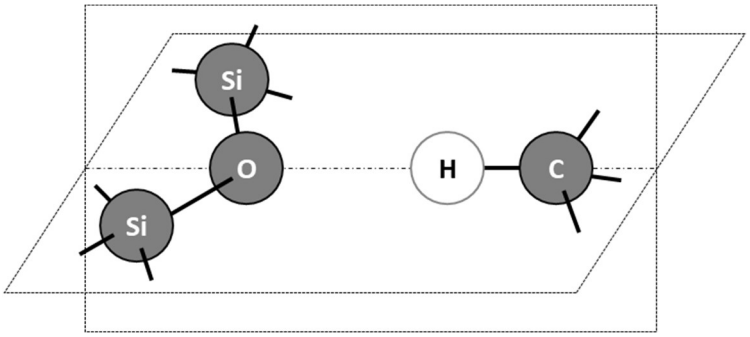

Scheme 1. Geometrical model for C, O and Si atoms involved in CH...O HBs extrapolated from COSi angle measurements on experimental structures.

In order to complete the conclusions drawn for the study of the experimental crystal structures, we have optimised by DFT-D3 a series of five selected OSDA-silica structures (**Table 1**). This representative series contains different FW types and F locations, and tetraalkylammonium or alkylimidizalium non-protonated cations $C_xH_yN_z^{n+}$ as OSDAs. In addition, one of the structures presents experimentally d_{CO} > 3.3 Å (STT). The DFT calculations, incorporating a London dispersion term (D3 approach[14]), will allow the positioning of the H atoms and an analysis of the properties of CH…O bonds. DFT functional and basis sets have been selected so as to yield the most realistic picture for the silica FW and the intermolecular interactions (**ESI 6**).

Table 1. Characteristics of OSDA-silica structures selected for the DFT-D study.

FW type	Pore channel dimensionality	F location	OSDA[a]
AST	0 D	$[4^6]$	TMA
TON	1 D	$[6^25^2]$	TMI
ITW	2 D	$[4^6]$	TMI
STT	2 D	$[5^44^3]$	TMAda
MFI	3 D	$[4^15^26^2]$	TPA

a. TMA (tetramethylammonium), TMI (1,3,4-trimethylimidazolium), TPA (tetrapropylammonium), TMAda (trimethyladamantanium).

We have first verified that the trends found for the CO distances and COSi angles in already published structures remain valid for the optimised structures (**ESI 7**). Second, we observe for these latter models that there are always small H-O distances (d_{HO} < 2.7 Å, below the sum of vdW radii[11]) and that they are related to large CHO angles (> 90°) (**Fig. 3**). The shorter these distances are, the closer to 150-180° the angles are. These are clear indications of the presence of weak but still directional CH...O HBs.[2, 13] When inspecting closely the geometry of the four shortest CH...O bonds for each OSDA-zeolite assembly, we found d_{HO} < 2.6 Å and CHO ≥ 126 ° for all structures (**ESI 8**). In addition, mean COSi angles are in the 100°-112° range containing the limit value of 106° discussed above. Furthermore, C, O and Si atoms are nearly coplanar. The atoms are out-of-plane at distances < 0.5 Å (often < 0.2 Å), and SiSiOC dihedral angles are between 115 and 175° (often > 140°), in global agreement with the extrapolated model obtained from crystal structures (**Scheme 1**). H atoms are close to be coplanar with C, H, O and Si atoms (out-of-plane distances < 0.6 Å). Further, we notice that the O atoms involved in these HBs are very often belonging to the silica cages containing F (8 over 20) or to the siloxane bonds directly attached to these cages (11 over 20). This evidences that charge distributions can play an important role in the formation of these weak HBs that are almost electrostatic in nature.[2, 15]

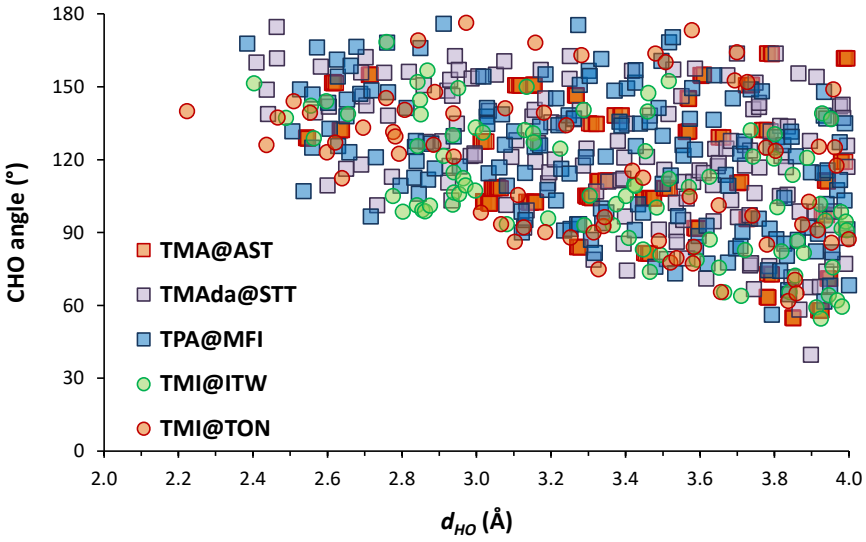

Fig. 3. CHO angles in optimised zeolite structures as a function of d_{HO} distances.

From Mulliken charge analysis (**ESI 9**), the silica FWs including F have a total charge close to -1, with F partial charges well above -1 (mean: -0.57 ±0.05). The latter slightly depend on the nature and strength of the F-Si interactions, covalent (-0.52 to -0.56 for F in large cages) or tetrel bonding (-0.66 for [4^6] cages). We notice also that O atoms have always negative partial charges around -1 (mean: -0.96 ±0.04). In the case of the OSDAs, N atoms bear negative charges (ca. -0.8 for tetraalkylammoniums and -0.5 for TMI) while the charge of C depends on its proximity to N. Significantly, all H - that are the peripheral atoms of the OSDAs - are always slightly positively charged (mean: +0.07 ±0.02). Therefore, the difference between H and O partial charges is equal or higher than +1. This high polarisation between the outer OSDAs' surfaces and O atoms of

the siloxane bonds strengthens the formation of HBs like in a charge-assisted process;[16] a strengthening already observed for organocations like tetramethylammonium.[17] It is also to note that the above distribution in partial charges is only valid for the OSDA-zeolite assembly. If the silica FW (with F) and the OSDA are considered separately (**ESI 9**), the siloxane bonds are less polarised with higher O partial charges (-0.62 ±0.03).

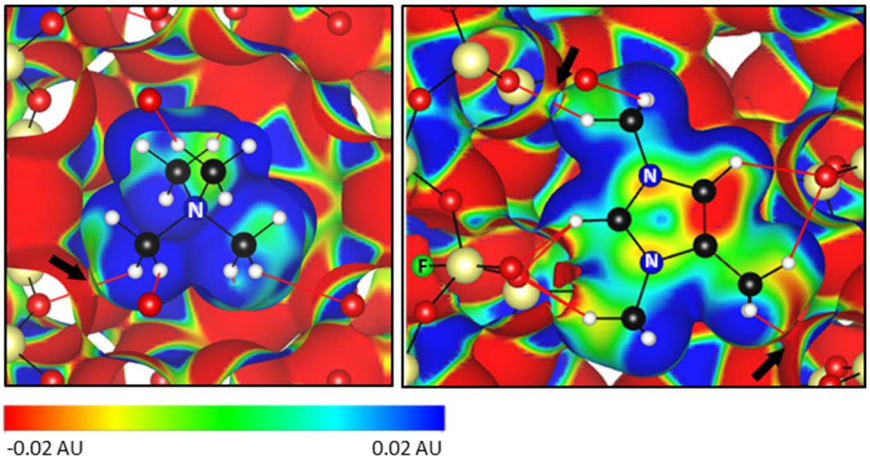

Fig. 4. Electrostatic potentials mapped on the electron charge density iso-surfaces (isovalue at 0.047 e.Å^{-3}) of TMA@AST and TMI@TON models. Surfaces have been cut so as to present the internal OSDA structure. Covalent bonds and HBs (d_{HO} < 2.7 Å) are represented as black and red lines. C, H, N, O, Si and F atoms are represented as balls using CPK convention (black, white, blue, red, yellow and green resp.)

We have calculated and plotted electron density maps coloured by the electrostatic potential (ESP) for the five modelled OSDA-zeolite assemblies (**ESI 10**). **Fig. 4** illustrates the typical hydrogen bonding schemes of tetraalkylammonium and imidazolium OSDAs, exemplified here by TMA@AST and TMI@TON assemblies. Several characteristics are noticeable. For the strongest HBs shown (d_{HO} < 2.7 Å), the electron charge density above 0.047 e.Å^{-3} does not vanish between H and O (e.g. black arrows in **Fig. 4**). In addition, there are significant contrasts between ESPs of the OSDAs (more positive) and the FWs (more negative). These contrasts exist at each side of the CH…O HBs, but they tend to equalize at their middle distance. When the donor (OSDA) and acceptor groups (O) are considered separately the differences in ESP are sharper, as appreciated for TMAda@STT in **ESI 11**. This observation can be related to the perturbing effect of HBs on the molecular electrostatic potentials.[18] If we have now a more global look to **Fig. 4**, we observe that mono- and bi-furcated HBs are anchoring the OSDAs inside the cage (AST) or the pore channel (TON). Reciprocally the OSDAs can be seen as attracting the silica tetrahedra around them.

These characteristics of CH…O HBs are valid for all modelled OSDA-zeolite assemblies. **Fig. 5** represents the H-bonding scheme around OSDAs for the strongest HBs (d_{HO} < 2.7 Å). Interestingly, these HBs are present in various directions and are connecting a high number of O atoms, equal or above the total number of C in OSDAs (from 6 to 15, **ESI 12**). This multiple anchoring originates in the high difference in charges existing

between all O and H atoms (*vide supra*). Meanwhile, other HBs can be formed when the OSDAs are subjected to dynamics. Using Born-Oppenheimer molecular dynamics simulations on a cluster model representative of the TPA@MFI assembly, we demonstrated recently this ability of the CH…O HBs to be continuously formed and disrupted depending on the competition between thermally activated OSDA motions and attractive HBs interactions.[10] The analysis of these dynamics lead then to distinguish between stable and instable (transitory) HBs. All these directional bonds coming from the outer surface of the OSDAs will collectively participate to the global stabilisation of the FW topology and to structure direction, along with the most usually considered Coulomb and vdW interactions.[19, 20]

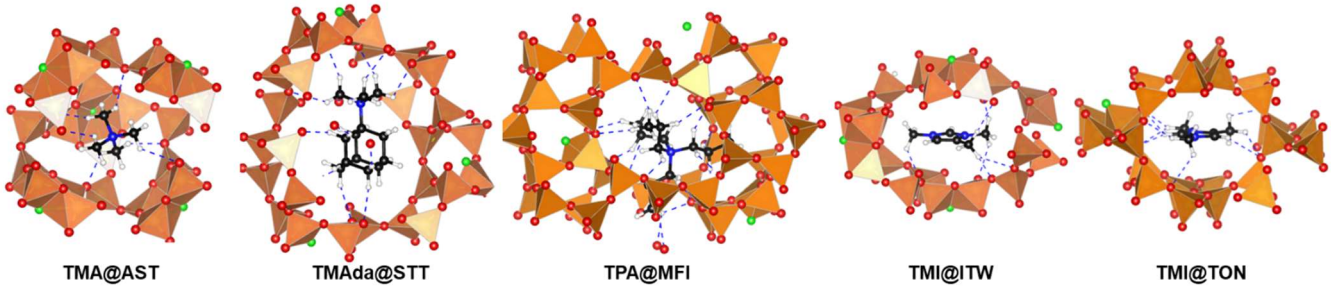

Fig. 5. Visualisation of CH…O HBs (d_{HO} < 2.7 Å, dashed lines) for the modelled OSDA-zeolite assemblies. Si atoms are represented at the centre of the polyhedra. C, H, N, O and F atoms are represented as balls using CPK convention (black, white, blue, red, green resp.).

In this communication, we have therefore demonstrated that CH…O hydrogen bonds between cationic OSDAs and silica FWs are ubiquitous for two series of 19+11 available experimental crystal structures presenting well-defined positions for C and N atoms of the OSDAs, and for Si and O atom of the FWs. A geometrical model for these HBs is extrapolated from the COSi and SiOSi angles measurements, showing a tendency to coplanarity for C, O and Si. The study of OSDA-zeolite assemblies using state-of-the-art DFT methods confirms these conclusions and shows the importance of the electrostatic interaction in the formation of these HBs. The OSDAs are anchored inside the cages or pore channels through multiple CH…O bonds thanks to the positive and negative charges beard by H and O atoms, respectively. Albeit weak when considered individually, these multiple and directional bonds participate thus to the stabilisation of the OSDA-zeolite assemblies, and have to be considered collectively when discussing the intermolecular interactions that drive zeolites' structure direction.

Acknowledgements

This work is supported by the CNRS, the French National Research Agency (ANR project ZEOORG), and the Algerian Bourses d'Excellence program. SA thanks EACEA for the Erasmus Mundus scholarship (program EM3E-4SW). KA and TM acknowledge the granted access by GENCI to the HPC resources of CCRT/CINES/IDRIS (allocation A0090807369).

Notes and references

‡ Cambridge Structural Database (CSD), Crystallography Open Database (COD), and International Zeolite Association's structure database (IZA).

§ For instance, evidence for CH…O formation ($d_{CO} \leq 3.3$ Å) was also obtained for the few silica-germania and AlPO zeolitic crystal structures found containing N based cationic OSDAs.

1. D. J. Sutor, *Nature*, 1962, **195**, 68.
2. G. R. Desiraju and T. Steiner, *The Weak Hydrogen Bond: In Structural Chemistry and Biology*, Oxford University Press Oxford, 2001.
3. G. R. Desiraju, *Acc. Chem. Res.*, 1996, **29**, 441.
4. M. C. Wahl and M. Sundaralingam, *Trends Biochem. Sci.*, 1997, **22**, 97.
5. O. Takahashi, Y. Kohno and M. Nishio, *Chem. Rev.*, 2010, **110**, 6049.
6. D. Braga, F. Grepioni and G. R. Desiraju, *Chem. Rev.*, 1998, **98**, 1375.
7. P. Behrens, G. vandeGoor and C. C. Freyhardt, *Angew. Chem. Int. Ed.*, 1996, **34**, 2680.
8. E. Dib, M. Freire, V. Pralong, T. Mineva and B. Alonso, *Acta Cryst. C*, 2017, **73**, 202.
9. C. M. Zicovich-Wilson, F. Gandara, A. Monge and M. Camblor, *J. Am. Chem. Soc.*, 2010, **132**, 3461.
10. T. Mineva, E. Dib, A. Gaje, H. Petitjean, J.-L. Bantignies and B. Alonso, *ChemPhysChem*, 2020, **21**, 149 .
11. A. Bondi, *J. Phys. Chem.*, 1964, **68**, 441.
12. E. Arunan, G. R. Desiraju, R. A. Klein, J. Sadlej, S. Scheiner, I. Alkorta, D. C. Clary, R. H. Crabtree, J. J. Dannenberg, P. Hobza, H. G. Kjaergaard, A. C. Legon, B. Mennucci and D. J. Nesbitt, *Pure Appl. Chem.*, 2011, **83**, 1637.
13. T. Steiner and G. R. Desiraju, *Chem. Commun.*, 1998, 891.
14. S. Grimme, J. Antony, S. Ehrlich and H. Krieg, *J. Chem. Phys.*, 2010, **132**, 154104.
15. T. Steiner, *Angew. Chem. Int. Ed.*, 2002, **41**, 48.
16. D. Braga and F. Grepioni, *Acc. Chem. Res.*, 2000, **33**, 601.
17. C. E. Cannizzaro and K. N. Houk, *J. Am. Chem. Soc.*, 2002, **124**, 7163.
18. M. D. Ryan, in *Modeling the Hydrogen Bond*, ed. D. Smith, Am. Chem. Soc., Washington, DC, 1994, ch. 4, pp. 36-59.
19. H. Gies and B. Marker, *Zeolites*, 1992, **12**, 42.
20. S. L. Burkett and M. E. Davis, *Chem Mater*, 1995, **7**, 920.